Structural Monitoring and Maintenance, *Vol. 7, No. 3 (2020) 195-213*
DOI: https://doi.org/10.12989/smm.2020.7.3.195

Identification of nonlinear systems through statistical analysis of the dynamic response

Marco Breccolotti*[1] and Chiara Pozzuoli[2a]

[1]*Department of Civil and Environmental Engineering, University of Perugia, via G. Duranti 93, Perugia, Italy*
[2]*RWDI, Via Thaon di Revel, 21, 20159, Milano, Italy*

(Received June 1, 2019, Revised May 14, 2020, Accepted August 9, 2020)

Abstract. In this paper an extension to the method for the identification of mechanical parameters of nonlinear systems proposed in Breccolotti and Materazzi (2007) for MDoF systems is presented. It can be used for damage identification purposes when damage modifies the linear characteristics of the investigated structure. It is based on the following two main features: the solution of the Fokker-Planck equation that describes the response probabilistic properties of the system when it is excited by external Gaussian loads; and a model updating technique that minimizes the differences between the response of the actual system and that of a parametric system used to identify the unknown parameters. Numerical analysis, that simulate virtual experimental tests, are used in the paper to show the capabilities of the method and to analyse the conditions required for its application.

Keywords: nonlinear systems; Gaussian excitation; Fokker-Planck equation; identification

1. Introduction

Most of the nowadays identification techniques, as reported for instance in the works by Doebling *et al.* (1996), Hoon *et al.* (2003) and in the special section of the IASC-ASCE Structural Health monitoring benchmark (Bernal and Beck 2004), are based on the determination of natural frequencies, modal shapes and damping even if other theories and methods are nowadays available (Li et al. 2014). These methods are suitable to study the damage represented by local cracks when it can be reasonably accepted the hypothesis that cracks are always open during the motion of the system (Patil and Maiti 2003, Lin *et al.* 2002, Kim and Stubbs 2003).

On the contrary, these methods are unreliable when the cracks, crossed by steel reinforcement, alternatively open and close during vibration, as it happens for instance in prestressed and reinforced concrete structures. This behaviour gives rise to changes in the dynamic response of the damaged structural element (Breccolotti *et al*. 2008).

The non-linearity of damaged reinforced concrete elements was recently studied jointly in the time-frequency domain by Owen *et al*. (2001) and by Neild *et al*. (2001). A finite element model for damaged reinforced concrete elements based on the theory of Fracture Mechanics was proposed by

*Corresponding author, Ph.D., E-mail: marco.breccolotti@unipg.it
[a] Ph.D., E-mail: chiara.pozzuoli@RWDI.com

http://www.techno-press.org/?journal=smm&subpage=7 ISSN: 2288-6605 (Print), 2288-6613 (Online)

Saavedra and Cuitino (2001). Also, Petryna and Krätzig (2005) proposed a procedure for the damage evaluation based on the strip modelling of prestressed and reinforced concrete structures. Other methods based on wavelet transformation and entropy measure have been recently proposed (Wimarshana *et al.* 2017).

Kalman filters have been also used for structural identification in the field of civil engineering. Wu and Smyth (2007) were among the first researcher to use unscented Kalman filter in this field highlighting its higher accuracy and robustness when dealing with structural identification of highly nonlinear systems compared to the extended Kalman filter. The improved performance of the unscented Kalman filter has been also observed by Chatzi and Smyth (2009) who exploited the potential of using heterogeneous (accelerations and displacements), non-collocated measurements for structural identification of a 3 DoF nonlinear system with a Bouc Wen hysteretic element. Efforts have been spent to overcome some limitations of this method, such as the complete knowledge of the input excitation (Lei *et al.* 2019), and to test its applicability to special cases such as structures equipped with Negative Stiffness Device (Erazo and Nagarajaiah 2018).

Recently, other techniques based on Markov chain Monte Carlo method (Green 2015) and on sparse regularization from input-output data (Lai and Nagarajaiah 2019a, b) have been proposed for system identification of structural systems with either nonlinear elastic or inelastic/hysteretic behavior.

To overcome some of the disadvantages of the existing dynamic methods, recent researches proposed the use of innovative techniques based on probabilistic analysis of the dynamic response of nonlinear structures subjected to Gaussian excitation. These methods rely on the property that the response of a nonlinear system to a Gaussian excitation is non-Gaussian. The upper statistical moments of the response are used as a measure of the non-gaussianity of the response and, therefore, as damage indicator.

The theoretical basis of this approach was studied by Cacciola and Muscolino (2002) and Cacciola *et al*. (2003). Subsequently, Hadjileontiadis *et al.* (2005) applied a similar methodology to a Plexiglas reduced-scale element, obtaining good results in the identification of structural parameters.

Numerical methods for the determination of approximate response probability function have been proposed in the past (Von Wagner and Wedig 2000, Iourtchenko *et al.* 2006, Mosbah and Fogli 2003). Identification of the parameters governing the dynamics of stochastically forced 1 DoF oscillators has been studied also by Boujo and Noiray (2017) and by Belenky *et al.* (2019). A MDoF system has been analyzed by Chen and Rui (2018).

In this paper the method based on the study by Breccolotti and Materazzi (2007) is extended and applied to several nonlinear MDoF systems for which a closed-form solution of the Fokker-Planck equation is available. Numerical analyses, that simulate virtual experimental tests, are used to show the capabilities of the method and emphasize the conditions required for its application.

2. Stochastic dynamics of MDoF nonlinear elastic systems

2.1 Theoretical background

Let us consider the following set of n equations for an *n*-DoF system, characterized by elastic nonlinear properties (Piszczec and Niziol 1986)

$$\ddot{x}_i + \beta_i \dot{x}_i + \frac{1}{m_i}\frac{\partial U}{\partial x_i} = f_i(t) \tag{1}$$

where $f_i(t)$ are stochastic processes with spectral density S_i and β_i are positive constants.

Through the substitutions $x_i = y_i$ and $\dot{x}_i = y_{i+n}$ this set can be re-written in the state space as a set of $2n$ first order differential equations

$$\dot{y}_i = y_{i+n} \tag{2}$$

$$\dot{y}_{i+n} = -\beta_i y_{i+n} - \frac{1}{m_i}\frac{\partial U}{\partial y_i} + f_i(t) \tag{3}$$

The term $U(y_1, y_2, ..., y_n)$ represents the potential energy of the system. It is further assumed that $f_i(t)$ are independent and uncorrelated white noises with null mean. From Eqs. (2) and (3) we can recognize that the coefficients of the Fokker-Planck's (FP) equation are given by

$$a_i = y_{i+n} \tag{4}$$

$$a_{i+n} = -\beta_i y_{i+n} - \frac{1}{m_i}\frac{\partial U}{\partial y_i} \tag{5}$$

$$b_{ij} = 0 \tag{6}$$

$$b_{i+n,j+n} = S_i \delta_{ij} \qquad i, j = 1, 2, ..., n \tag{7}$$

The diffusion equation becomes

$$\frac{1}{2}\sum_{i=1}^{n} S_i \frac{\partial^2 w}{\partial y_{i+1}^2} - \sum_{i=1}^{n} S_i \frac{\partial}{\partial y_i}(y_{i+n} w) + \sum_{i=1}^{n} S_i \frac{\partial}{\partial y_{i+n}}\left[\left(\beta_i y_{i+n} + \frac{1}{m_i}\frac{\partial U}{\partial y_i}\right) w\right] = 0 \tag{8}$$

where the probability density function $w(y_1, ..., y_n, y_{n+1}, ..., y_{2n})$ depends on the $2n$ variables. Eq. (8) can then be re-written as

$$\sum_{i=1}^{n}\left[\left(\beta_i \frac{\partial}{\partial y_{i+n}} - \frac{\partial}{\partial y_i}\right)\left(y_{i+n} w + \frac{S_i}{2\beta_i}\frac{\partial w}{\partial y_{i+n}}\right)\right] + \sum_{i=1}^{n}\left[\frac{\partial}{\partial y_{i+n}}\left(\frac{1}{m_i}\frac{\partial U}{\partial y_i} w + \frac{S_i}{2\beta_i}\frac{\partial w}{\partial y_i}\right)\right] = 0 \tag{9}$$

This equation can be solved assuming the validity of the following conditions

$$\frac{S_i m_i}{2\beta_i} = k \qquad i = 1, 2, ..., n \tag{10}$$

being k a positive constant. In this case the solution of the FP equation is

$$w(y_1,...,y_n,y_{n+1},...,y_{2n}) = C\exp\left[-\frac{1}{k}\left(\frac{1}{2}\sum_{i=1}^{n} m_i y_{i+n}^2 + U\right)\right] \tag{11}$$

This form of the probability density function is known as the Maxwell-Boltzmann distribution, being the expression inside the parentheses the total mechanical energy of the system

$$U_c = E + U = \frac{1}{2}\sum_{i=1}^{n} m_i \dot{x}_i^2 + U(x_1,...,x_n) \tag{12}$$

Then, the response probability density function can be written as

$$w(x_1,...,x_n,\dot{x}_1,...,\dot{x}_n) = C\exp\left[-\frac{1}{k}U_c\right] \tag{13}$$

From Eqs. (12) and (13) it can be seen that the velocity probability density function is Gaussian.

The joint probability density function w can also be expressed as the product of two terms, separating the random quantities displacement x_i xi and velocity $\dot{x}_i$. Thus, the displacement probability density function is given by

$$w(x_1,...,x_n) = C_1\exp\left[-\frac{1}{k}U\right] \tag{14}$$

where C_1 is a normalizing constant

3. Stochastic identification

3.1 General procedure

The identification of the mechanical parameters (stiffness and damping) of real structures can be performed by solving an inverse problem of stochastic dynamics. In this section an identification procedure, which relies on the theoretical basis recalled in the previous section, is presented. The method is composed of several phases that can be briefly described as follows:

(i) Excitation of the system. The physical system is excited by *n* band-limited white noises $f_1(t),..., f_n(t)$, statistically independent and characterized by constant power spectra $S_{01},...,S_{0n}$, which meet the condition expressed by Eq. (10). Excitations of this type can be generated, for instance, through electrodynamic shakers with a closed loop control system.

(ii) Measure of the system response. The proposed procedure requires that the response of the system in terms of displacements $x_1(t),...,x_n(t)$ is known through measurements.

(iii) Identification of the parameters that describe the nonlinear elastic stiffnesses. Having assumed for the nonlinear stiffnesses a prescribed law, the identification of the elastic behavior of the system corresponds to the determination of a set of unknown parameters that minimizes the functional

$$J = \int_{-\infty}^{+\infty} \left[w_{test}\left(x_1,...,x_n\right) - w_{fpe}\left(x_1,...,x_n\right) \right]^2 dx_1...dx_n \tag{15}$$

where $w_{test}\left(x_1,...,x_n\right)$ indicates the probability density function of the measured data, and $w_{fpe}\left(x_1,...,x_n\right)$ indicates the probability density function obtained by placing tentative values of the unknown variables in the parametric solution of the FP equation. Since the system response is known by measurements at discrete times, the functional *J* used in the identification algorithm (Eq. (15)) has to be calculated through finite values, summing the squared differences between the measured and the theoretical relative frequencies

$$J = \sum_{i_1=1}^{p} ... \sum_{i_n=1}^{p} \left[\frac{N_{test,i_1...i_n}}{N_{tot}} - \frac{N_{x_i...x_n}\left(x_i...x_n\right)}{N_{tot}} \right]^2 \tag{16}$$

where *p* is the number of intervals used in the determination of the relative frequencies;

N_{tot} is the total number of the sampled measurements, each of which is represented by the values $x_i\left(t\right),...,x_n\left(t\right)$ at the generic time *t*;

$\frac{N_{test,i_1...i_n}}{N_{tot}}$ indicates the relative frequency of experimental data;

$\frac{N_{x_i...x_n}\left(x_i...x_n\right)}{N_{tot}}$ indicates the theoretical relative frequencies of the system response obtained solving the FP equation.

3.2 Genetic algorithms

Genetic algorithms have been chosen to solve the optimization problem for their capabilities in finding global minimum rather than local minimum and for the possibility of taking into account nonlinear constraints. Given the general objective functional

$$J\left(\boldsymbol{x}\right), \qquad \boldsymbol{x} = \left[x_1,...,x_n\right] \in ¡^{\,n} \tag{17}$$

defined within the area of search $S \subseteq \mathbb{R}^n$, the optimal solution is the one to which corresponds the minimum (or maximum) of the objective functional *J*. The genetic algorithm, after its initialization, randomly generates populations of the unknown parameters that represent potential solutions of the optimization problem. The functional *J* is evaluated for each individual of each population. The individuals that obtained the best values of the functional *J* are selected for the next generation. Other individuals are selected on the basis of their performances as parent individual. They are used in crossover and mutation operations to generate further individuals. In addition, further individuals are randomly generated and included in the next generation. The algorithm ends when the performance of one individual is close enough to the target performance.

Usually the searching space *S* is represented through a *n*-dimensional hyperspace defined by the upper and lower limits of each variable

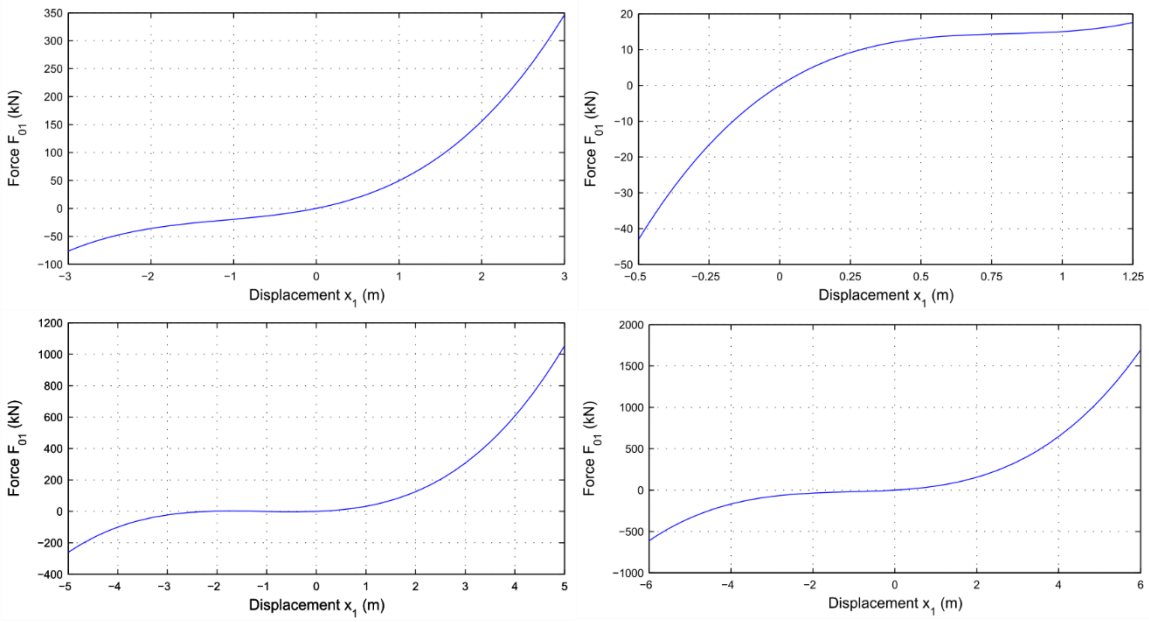

Fig. 1 Stiffness laws used for spring 1 in numerical models of Examples 1 (top left), 2 (top right), 3 (bottom left) and 4 (bottom right)

$$x_{i,\min} < x_i < x_{i,\max} \qquad for \quad i = 1,...,n \tag{18}$$

Eventually, in a region $F \subseteq S$ the following m equality or inequality constraints have to be fulfilled

$$g_i(\boldsymbol{x}) \le 0 \quad for \quad i = 1,...,q \qquad \text{and} \qquad h_i(\boldsymbol{x}) = 0 \quad for \quad i = q+1,...,m \tag{19}$$

In this context local optimization methods, such as the method of gradient, ensure convergence only in a local minimum and are much more sensitive to the point where the algorithm is started. Conversely, evolutionary algorithms, widely used since the publication of the book by Goldberg (1989), are particularly suitable for solving constrained non-convex optimization problems.

4. Numerical examples

4.1 General remarks

The validity of the identification procedure described in the previous paragraph has been tested by carrying out several numerical simulations on 2-DoF and 5-DoF systems.

Different behaviors have been assumed for the nonlinear spring as shown in Fig. 1.

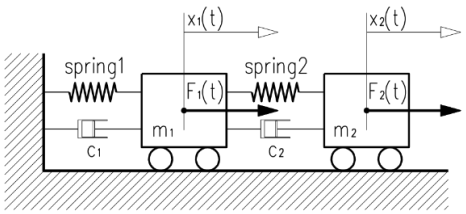

Fig. 2 Two DoF nonlinear elastic system

4.2 Example 1: 2-DoF nonlinear elastic system with increasing stiffness

A 2-DoF system characterized by masses m_1 and m_2, damping coefficients c_1 and c_2 and stiffnesses parameters $k_1(x)$ and $k_2(x)$ is considered (Fig. 2). The spring #1 is nonlinear elastic and the relationship between force F_{e1} and displacement x_1 is expressed by

$$F_{e1}(x_1) = k_1\left[x_1 + G_1(x_1)\right] \tag{20}$$

being

$$G_1(x_1) = b_1 x_1^2 + a_1 x_1^3 \tag{21}$$

and where the coefficients a_1 and b_1 are constant. The spring #2 is linear elastic and the relationship between the force F_{e2} and relative displacement $x_2 - x_1$ is expressed by

$$F_{e2}(x_2 - x_1) = k_2(x_2 - x_1) \tag{22}$$

The external forces $F_1(t)$ and $F_2(t)$, acting on the masses m_1 and m_2, are band limited white noises.

The FP equation can be obtained from the following dynamic equilibrium equations

$$\begin{aligned} &m_1\ddot{x}_1 + c_1\dot{x}_1 + c_2(\dot{x}_1 - \dot{x}_2) + k_1\left(x_1 + b_1x_1^2 + a_1x_1^3\right) + k_2(x_1 - x_2) = F_1(t) \\ &m_2\ddot{x}_2 + c_2(\dot{x}_2 - \dot{x}_1) + k_2(x_2 - x_1) = F_2(t) \end{aligned} \tag{23}$$

which can also be written, in matrix form, as

$$\begin{aligned} &\begin{bmatrix} m_1 & 0 \\ 0 & m_2 \end{bmatrix}\begin{Bmatrix} \ddot{x}_1 \\ \ddot{x}_2 \end{Bmatrix} + \begin{bmatrix} (c_1 + c_2) & -c_2 \\ -c_2 & c_2 \end{bmatrix}\begin{Bmatrix} \dot{x}_1 \\ \dot{x}_2 \end{Bmatrix} + \\ &+\begin{bmatrix} (k_1 + k_2) & -k_2 \\ -k_2 & k_2 \end{bmatrix}\begin{Bmatrix} x_1 \\ x_2 \end{Bmatrix} + \begin{Bmatrix} k_1\left(b_1x_1^2 + a_1x_1^3\right) \\ 0 \end{Bmatrix} = \begin{Bmatrix} F_1(t) \\ F_2(t) \end{Bmatrix} \end{aligned} \tag{24}$$

It is assumed that the damping matrix can be expressed, in accordance with the Rayleigh's

hypothesis, as

$$[C]=\beta[M]+\alpha[K] \tag{25}$$

where, for the sake of simplicity, it has been assumed $\alpha=0$. After some algebra, Eq. (23) becomes

$$\begin{aligned}&\ddot{x}_1+\beta\dot{x}_1+\frac{1}{m_1}\left[\left(k_1+k_2\right)x_1-k_2x_2+k_1\left(x_1+b_1x_1^2+a_1x_1^3\right)\right]=f_1(t)\\&\ddot{x}_2+\beta\dot{x}_2+\frac{1}{m_2}\left(-k_2x_1+k_2x_2\right)=f_2(t)\end{aligned} \tag{26}$$

Recalling Eq. (1), the potential energy of the system can be found

$$U\left(x_1,x_2\right)=-k_2x_1x_2+k_2\frac{x_2^2}{2}+k_1\frac{x_1^2}{2}+k_2\frac{x_1^2}{2}+k_1\frac{b_1x_1^3}{3}+k_1\frac{a_1x_1^4}{4}+c \tag{27}$$

The constant *c* has to be determined taking into account the initial condition of the system. Since the stochastic process $F_i(t)$ is characterized by a constant spectral density from $-\infty$ to $+\infty$ equal to S_{0i}, the corresponding scaled stochastic process $f_i(t)=\frac{F_i(t)}{m_i}$, will have a constant spectral density equal to

$$S_{0i\_m}=\frac{S_{0i}}{m_i^2} \tag{28}$$

The diffusion equation becomes

$$\sum_{i=1}^{2}\left[\left(\beta\frac{\partial}{\partial x_{i+n}}-\frac{\partial}{\partial x_i}\right)\left(x_{i+n}w+\frac{S_{0i\_m}}{2\beta}\frac{\partial w}{\partial x_{i+n}}\right)\right]+\sum_{i=1}^{2}\left[\frac{\partial}{\partial x_{i+n}}\left(\frac{1}{m_i}\frac{\partial U}{\partial x_i}w+\frac{S_{0i\_m}}{2\beta}\frac{\partial w}{\partial x_i}\right)\right]=0 \tag{29}$$

but the problem can be solved only under the following conditions (see Eq. (10))

$$\frac{S_{0i\_m}\cdot m_i}{2\beta}=k \qquad for \quad i=1,2 \tag{30}$$

The solution of the FP equation in terms of the displacements PDF can be written as

$$w_1\left(x_1,x_2\right)=C_1\exp\left[-\frac{1}{k}\left(-k_2x_1x_2+k_2\frac{x_2^2}{2}+k_1\frac{x_1^2}{2}+k_2\frac{x_1^2}{2}+k_1\frac{b_1x_1^3}{3}+k_1\frac{a_1x_1^4}{4}\right)\right] \tag{31}$$

where C_1 is a constant. To satisfy the condition expressed by Eq. 30 the value of the forcing PSD has to be appropriately tuned imposing that

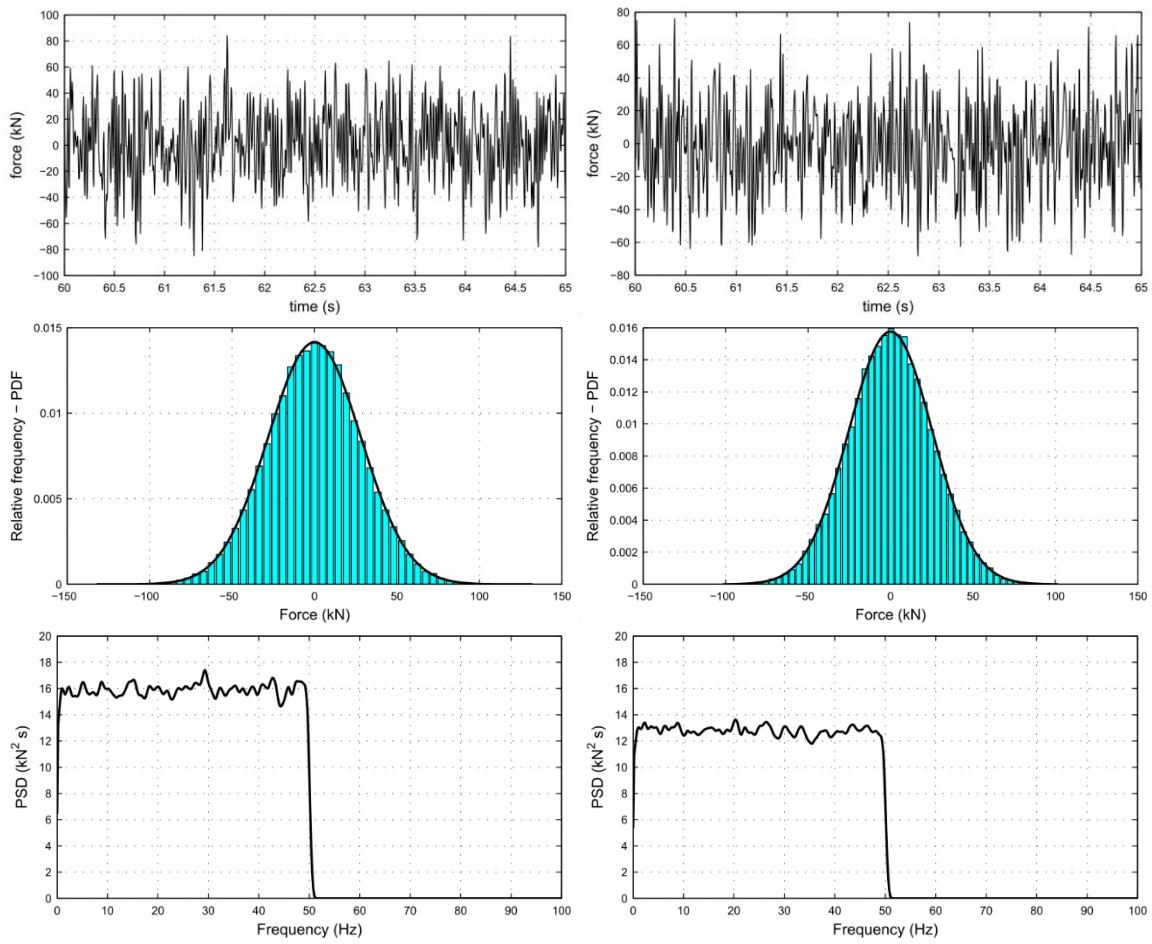

Fig. 3 Samples of the time histories with relative frequencies and power spectrum densities of the band limited white noises used in Examples 1 and 2. The left-hand column is related to node n. 1, while the second column refers to node n. 2

$$\frac{S_{01\_m} \cdot m_1}{2\beta} = \frac{S_{02\_m} \cdot m_2}{2\beta} = k \tag{32}$$

The coefficient β, which multiplied by the mass matrix provides the damping matrix of the system, has been chosen so that the damping rate for the second vibration mode is equal to 5% of critical.

The first numerical model considered in this investigation is made up of two masses, m_1 and m_2, respectively equal to 400 kg and 320 kg. The masses are subject to the action of external Gaussian forces having power spectral densities S_{01} and S_{02} equal to 16.0 kN^{2}m and 12.8 kN^{2}m, respectively. The forces time histories have been generated in the frequency range 0.1 - 50.1 Hz using the well-known algorithm proposed by Shinozuka and Jan (1972). From the analysis of Fig.

3, where the time histories, PDF and PSD of the forces are shown, it is possible to see that effectively the generated time histories well represent the two desired band limited white noise processes. The behavior of the nonlinear spring #1 is described by Eqs. (20) and (21) with $k_1 = 30$ kN/m, $a_1 = 0.15$ m^{-2} and $b_1 = 0.5$ m^{-1}. The hardening elastic behavior is represented in Fig. 1. The spring #2 is characterized by constant stiffness equal to $k_2 = 40$ kN/m.

The duration of the process is 300 sec, with a sampling rate of 200 Hz. The displacement, the velocity and the acceleration time histories have been numerically evaluated by direct integration of the equations of motion using the HHT algorithm (Hughes 1987). The histograms of the calculated displacements for the 2 nodes are shown in Fig. 4.

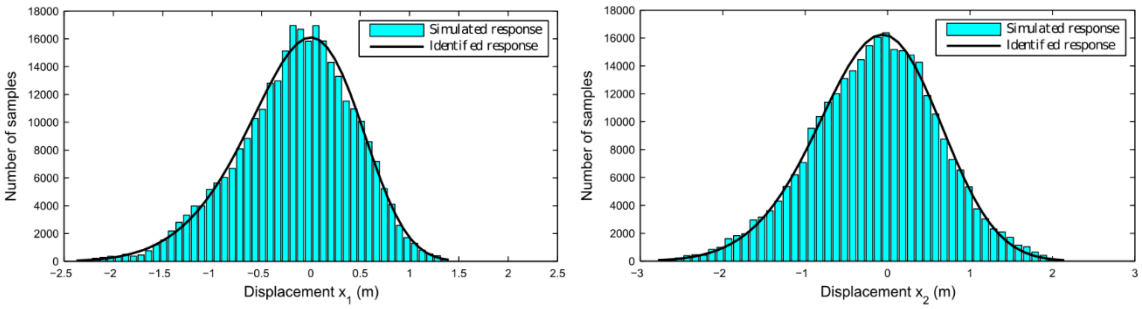

Fig. 4 Example 1: Comparison between experimental (bars) and identified (lines) displacements PDFs for node n. 1 (left) and node n. 2 (right)

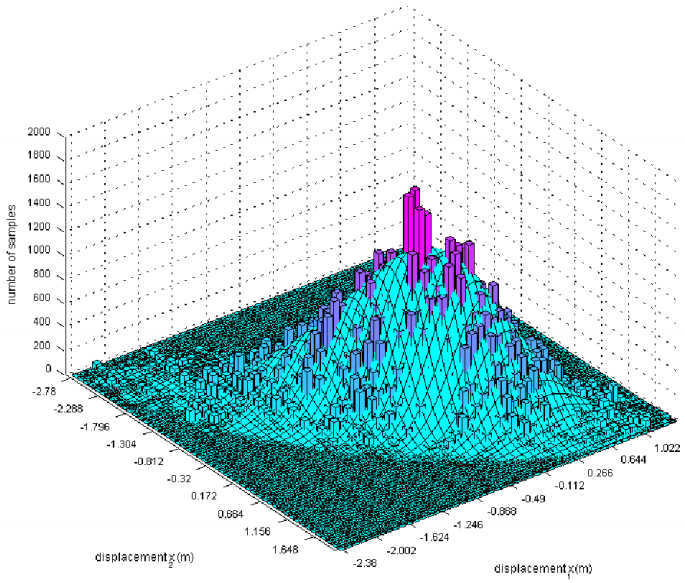

Fig. 5 Example 1: Comparison between experimental (bars) and identified (surface) displacements joint PDF

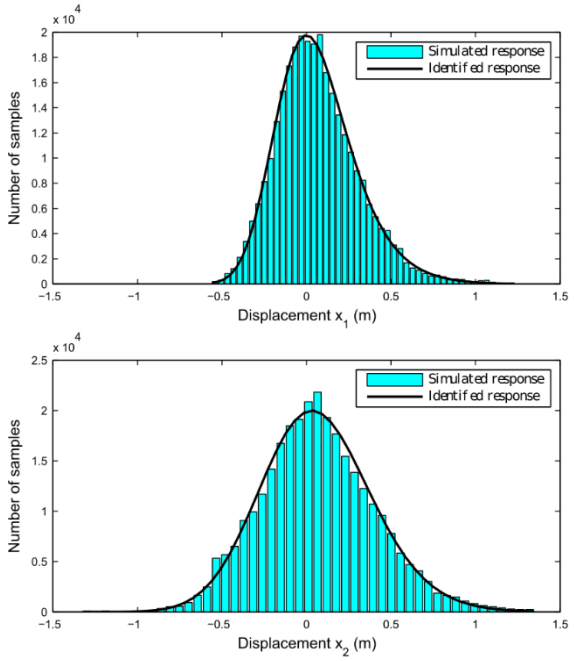

Fig. 6 Example 2: Comparison between experimental (bars) and identified (lines) displacements PDFs for node n. 1 (left) and node n. 2 (right)

Applying the procedure proposed in Section 3 the following unknown parameters have been identified: $k_1^{id} = 28.25\,kN/m$, $a_1^{id} = 0.155\,m^{-2}$, $b_1^{id} = 0.502\,m^{-1}$ and $k_2^{id} = 41.5\,kN/m$. with relative errors equal to 5.8%, 3.3%, 0.4% and 3.7%. The theoretical PDFs corresponding to the identified parameters are also shown in Fig. 4. The comparison between experimental and identified displacements joint PDF is shown in Fig. 5.

4.3 Example 2: 2-DoF nonlinear elastic system with decreasing stiffness

The second numerical model considered is similar to the first one with masses m_1 and m_2, respectively equal to 400 kg and 320 kg, subjected to the same external forces used in the previous example. The behavior of the nonlinear spring #1, described by Eqs. 20-21 with k_1 = 50 kN/m, a_1 = 0.5 m^{-2} and b_1 = −1.2 m^{-1}, is of softening type (Fig. 1). The spring #2 is characterized by a constant stiffness k_2 equal to 40 kN/m. The histograms of the calculated displacements for the 2 nodes are shown in Fig. 6. With the proposed procedure the following unknown parameters have been identified: $k_1^{id} = 49.875\,kN/m$, $a_1^{id} = 0.525\,m^{-2}$, $b_1^{id} = -1.300\,m^{-1}$ and $k_2^{id} = 41.0\,kN/m$.

Also in this case the relative errors turned out quite small being equal to -0.2%, 5.0%, 3.7% and 2.5%, respectively. The theoretical PDFs corresponding to the identified parameters are shown in Fig. 6 while the comparison between experimental and identified displacements joint PDF is shown in Fig. 7.

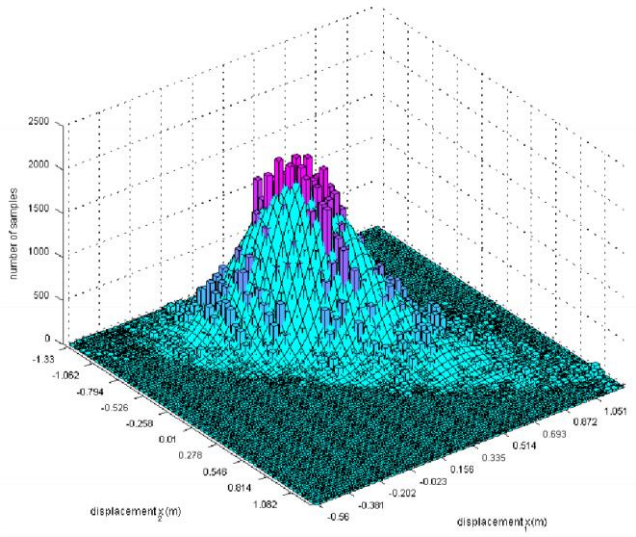

Fig. 7 Example 2: Comparison between experimental (bars) and identified (surface) displacements joint PDF

4.4 Example 3: 2-DoF nonlinear elastic system with asymmetric increasing stiffness

The third numerical model analyzed is still a 2-DoF system with masses m_1 and m_2, respectively equal to 312.5 kg and 250 kg. The two masses are subjected to the action of external Gaussian forces having power spectral densities S_{01} and S_{02} equal to 9.0 kN^{2}m and 7.2 kN^{2}m, respectively, in the frequency range 0.1 - 50.1 Hz. The time histories, PDF and PSD of the applied forces are shown in Fig. 8. The behavior of the nonlinear spring #1, described by Eqs. (20) and (21) with k_1 = 12 kN/m, a_1 = 0.398 m^{-2} and b_1 = 1.32 m^{-1}, is of asymmetric hardening type (Fig. 1). The spring #2 is characterized by constant stiffness k_2 equal to 50 kN/m. The results of the numerical integration are shown with histogram bars in Figs. 9. The unknown parameters have been identified with the optimization technique based on genetic algorithm described in sec. 4.4. The optimal solution has been searched carrying out 3000 generations each having a population of 100 vectors of the four unknowns k_1, a_1, b_1, k_2. For each parameter the solution has been searched in a range corresponding to ±50% the true value. The convergence of the fitness function to the optimal solution as the number of generation increases is shown in Fig. 10. The proposed method allowed the identification of the following unknown parameters: $k_1^{id} = 11.798\, kN/m$, $a_1^{id} = 0.405\, m^{-2}$, $b_1^{id} = 1.330\, m^{-1}$ and $k_2^{id} = 52.395\, kN/m$.

The theoretical probability density functions corresponding to these identified values are shown in Fig. 9 with solid curves. The experimental and the identified displacements joint PDFs are shown in Fig. 11.

In order to assess the robustness of the method to real life experimental conditions, each response has been contaminated by fictitious noises. Uniformly distributed disturbances with zero mean and noise-to-signal ratio up to ±1% and ±5% have been added to the pseudo experimental displacement data.

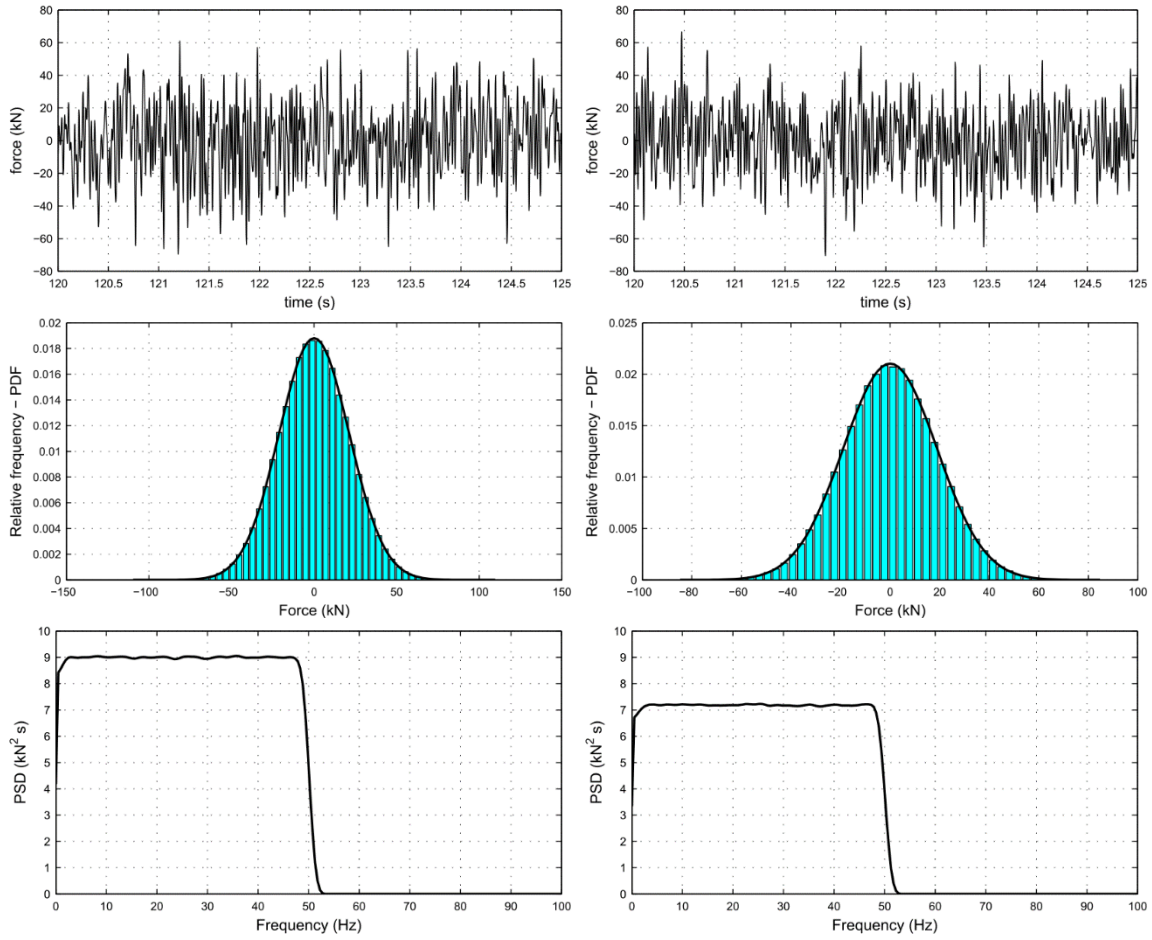

Fig. 8 Example 3: Samples of the time histories with relative frequencies and power spectrum densities of the band limited white noises. The left-hand column is related to node n. 1, while the second column refers to node n. 2

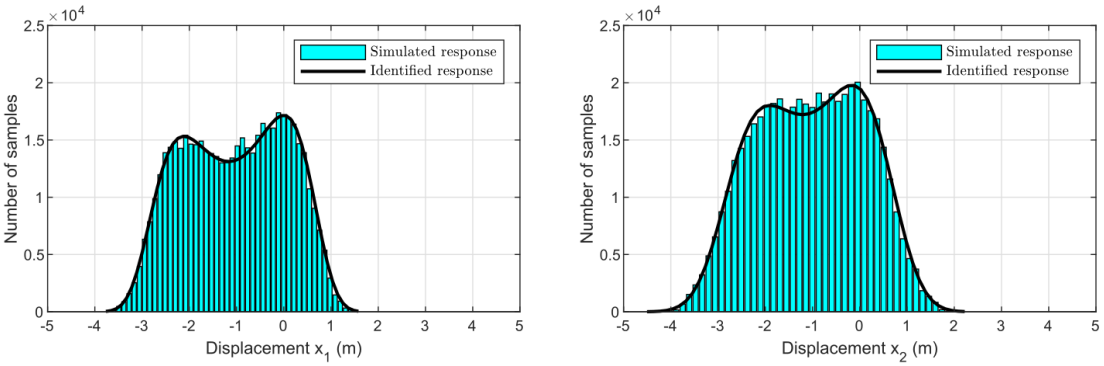

Fig. 9 Example 3: Comparison between experimental (bars) and identified (lines) displacements PDFs for node n. 1 (left) and node n. 2 (right)

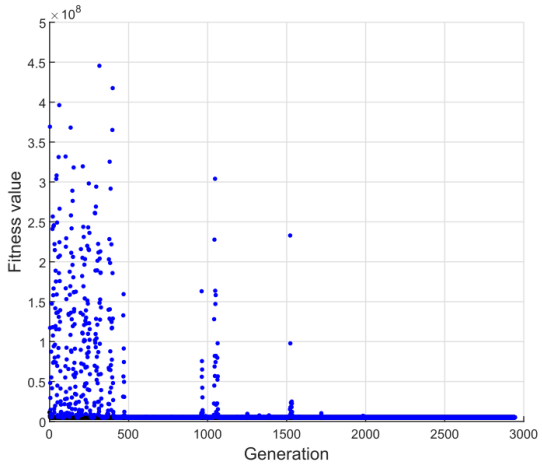

Fig. 10 Example 3: Convergence of the genetic algorithm solution to the optimal one

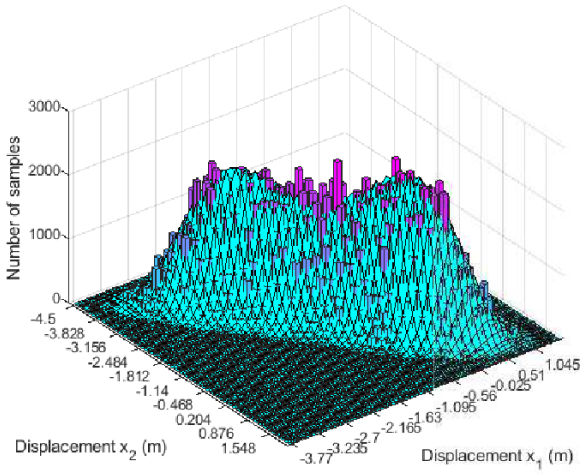

Fig. 11 Example 3: Comparison between experimental (bars) and identified (surface) displacements joint PDF

Table 1 Example 3: Results of identification with and without noise

			Without noise		1% noise		5% noise	
Parameter		True	Identified	Error (%)	Identified	Error (%)	Identified	Error (%)
k_1	(kN/m)	12.0	11.80	-1.7	11.81	-1.6	11.78	-1.8
a_1	(m^{-2})	0.398	0.405	-1.8	0.405	-1.8	0.405	-1.8
b_1	(m^{-1})	1.32	1.330	+0.8	1.330	+0.8	1.327	+0.5
k_2	(kN/m)	50.0	52.39	+4.8	52.35	+4.7	51.01	+2.0

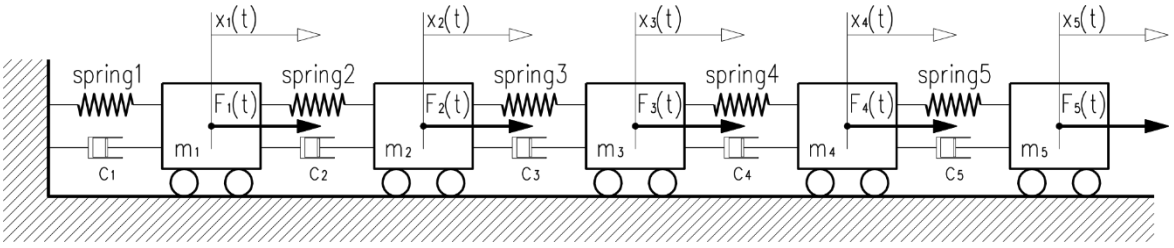

Fig. 12 Example 4: Five DoF nonlinear system

In the case of noises with 1% noise-to-signal ratio the following unknown parameters have been identified: $k_1^{id} = 11.806\,kN/m$, $a_1^{id} = 0.405\,m^{-2}$, $b_1^{id} = 1.330\,m^{-1}$ and $k_2^{id} = 52.355\,kN/m$.

Similarly, for 5% noises the identified parameters turned out to be: $k_1^{id} = 11.784\,kN/m$, $a_1^{id} = 0.405\,m^{-2}$, $b_1^{id} = 1.327\,m^{-1}$ and $k_2^{id} = 51.014\,kN/m$. The complete results are also reported in Table 1 for comparison purposes.

4.5 Example 4: 5-DoF nonlinear elastic system

The proposed procedure has been finally applied to a 5 DoF system (Fig. 12) with masses m_1, m_2, m_3, m_4 and m_5 respectively equal to 400 kg, 320 kg, 250 kg, 200 kg and 150 kg. External zero mean Gaussian forces having power spectral densities S_{01}, S_{02}, S_{03}, S_{04} and S_{05} equal to 16.0 kN^{2}m, 14.3 kN^{2}m, 12.65 kN^{2}m, 11.31 kN^{2}m and 9.80 kN^{2}m have been applied to these masses. The behavior of nonlinear spring #1, described by Eqs. (20) and (21) with k_1 = 30 kN/m, a_1 = 0.15m^{-2} and b_1 = 0.50 m^{-1}, is of asymmetric hardening type (Fig. 1). The remaining springs are characterized by constant stiffness equal to $k_2 = k_3 = k_4 = k_5 = 40$ kN/m.

The displacements distributions obtained by integration for the 5 DoF are shown in Fig. 13. For this system the potential energy U is equal to

$$U(x_1, x_2) = \sum_{i=1}^{5} k_i \frac{x_i^2}{2} + \sum_{i=1}^{4} k_{i+1} \frac{x_i^2}{2} - \sum_{i=1}^{4} k_{i+1} x_i x_{i+1} + k_1 \frac{b_1 x_1^3}{3} + k_1 \frac{a_1 x_1^4}{4} \tag{33}$$

The mathematical development accomplished in Section 4.2 is also valid for a 5 DoF system. Consequently, an identification procedure similar to the one used for 2 DoF systems can be adopted to identify the unknown parameters of the mechanical system. By doing so, the following values of the mechanical parameters have been identified: $k_1^{id} = 31.121\,kN/m$, $a_1^{id} = 0.142\,m^{-2}$ and $b_1^{id} = 0.503\,m^{-1}$ for the nonlinear spring and $k_2^{id} = 37.744\,kN/m$, $k_3^{id} = 38.769\,kN/m$, $k_4^{id} = 36.641\,kN/m$ and $k_5^{id} = 36.360\,kN/m$ for the linear springs.

The relative errors committed in this identification are shown in Table 2. The comparison between the displacement's distributions calculated by means of numerical simulation and the distributions corresponding to the identified parameters is shown in Fig. 13.

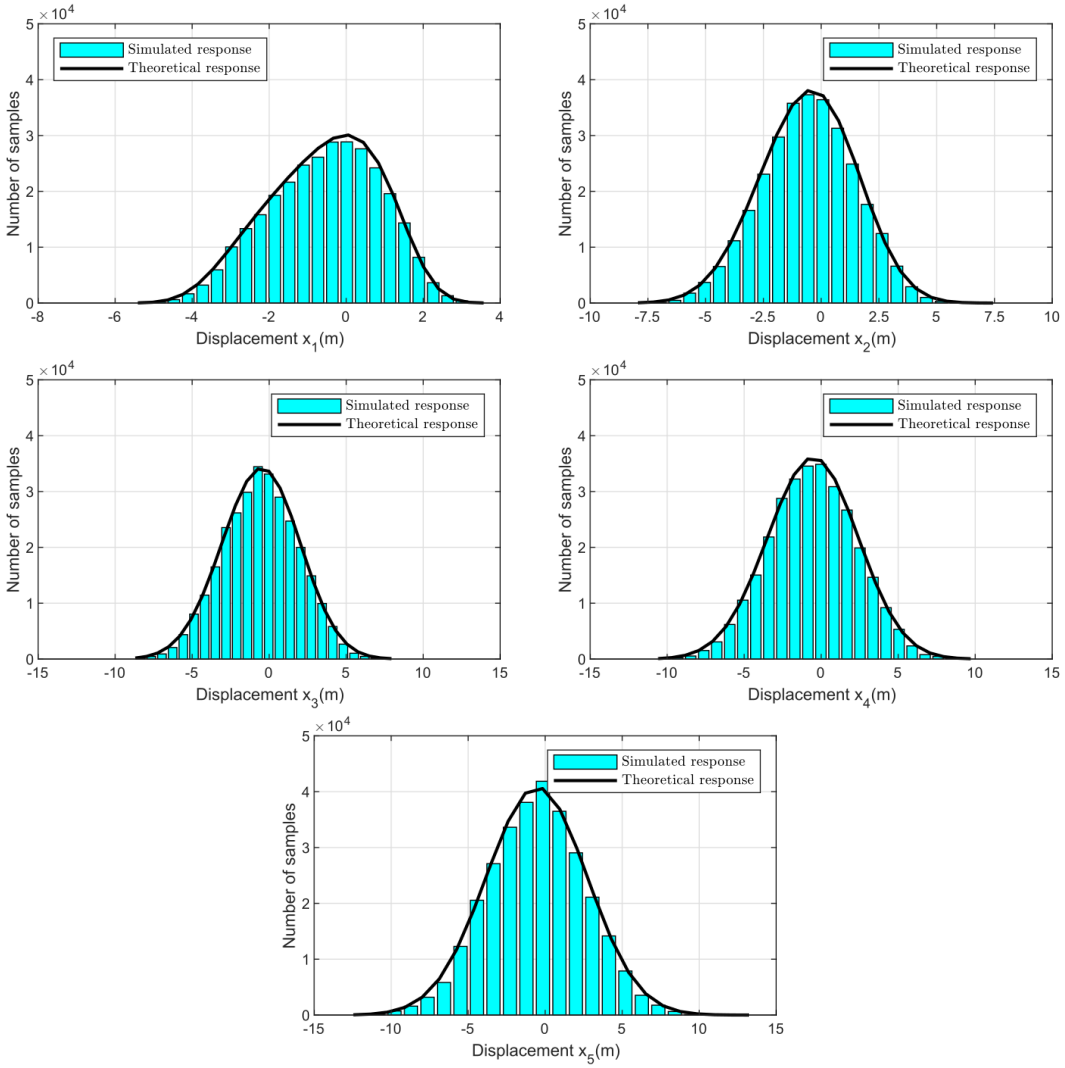

Fig. 13 Example 4: Comparison between experimental (bars) and identified (lines) displacements PDFs for the 5 nodes

Also in this case, artificially generated noises have been added to the pseudo-experimental data to verify the robustness of the method. For the case of 1% noise-to-signal ratio, the following unknown parameters have been identified: $k_1^{id} = 31.384\,kN/m$, $a_1^{id} = 0.138\,m^{-2}$, $b_1^{id} = 0.496\,m^{-1}$, $k_2^{id} = 37.722\,kN/m$, $k_3^{id} = 38.684\,kN/m$, $k_4^{id} = 36.610\,kN/m$ and $k_5^{id} = 36.381\,kN/m$.

Afterwards, adding noise up to 5% the following unknown parameters have been identified: $k_1^{id} = 31.421\,kN/m$, $a_1^{id} = 0.138\,m^{-2}$ and $b_1^{id} = 0.495\,m^{-1}$ for the nonlinear spring and $k_2^{id} = 37.820\,kN/m$, and $k_3^{id} = 38.519\,kN/m$, $k_4^{id} = 36.383\,kN/m$ and $k_5^{id} = 35.820\,kN/m$ for the other springs. The accuracy of these estimates is shown in Table 2.

Table 2 Example 4: Results of identification with and without noise

Parameter		True	Without noise		1% noise		5% noise	
			Identified	Error (%)	Identified	Error (%)	Identified	Error (%)
k_1	(kN/m)	30.0	31.12	+3.7	31.38	+4.6	31.42	+4.7
a_1	(m^{-2})	0.15	0.142	-5.3	0.138	-8.0	0.138	-8.0
b_1	(m^{-1})	0.50	0.503	+0.6	0.496	-0.8	0.495	-1.0
k_2	(kN/m)	40.0	37.74	-5.6	37.72	-5.7	37.82	-5.4
k_3	(kN/m)	40.0	38.77	-3.1	38.68	-3.3	38.52	-3.7
k_4	(kN/m)	40.0	36.64	-8.4	36.61	-8.5	36.38	-9.0
k_5	(kN/m)	40.0	36.36	-9.1	36.38	-9.0	35.82	-10.4

4.5 Comments on the obtained results

The results of the numerical simulations presented in the previous paragraphs provide evidence of the ability of the proposed method in identifying different types of non-linearity. Several numerical investigations also proved the robustness of the method against experimental noises with noise-to-signal ratio up to 5%. In particular, this was all the more true for the parameters that describe the non-linearity of the system, which represent the most interesting data of the investigation. It should, however, be recalled that the applicability of the method requires the occurrence of specific conditions. First of all, the theory underlying the proposed method foresees the elasticity of the system also in the nonlinear field. Thus, the method cannot be used to identify hysteretic behaviors for which other methods must be referred to. Secondly, the method requires compliance with Eq. 10 which can certainly lead to organizational problems. In fact, it requires that all degrees of freedom be loaded simultaneously with forces having predetermined spectral density values. This condition can be achieved, for example, by using different electrodynamic shakers or can occur in the case of structural system with equal masses subjected to uniform excitations.

5. Conclusions

In this paper a new methodology for the structural identification of nonlinear system has been introduced. It is based upon the solution of the Fokker-Planck equation. One of its main advantage is that it only requires the knowledge of the statistical properties of the external forces applied to the system without the need of knowing their exact time histories. The method is composed of three different phases: system excitation with band-limited white noise; solution, in a parametric form, of the Fokker-Planck equation that describes the response of the structure; identification of the system unknown parameters by minimizing an appropriate functional. The identification method has been validated through numerical simulations carried out on two- and five-degrees of freedom systems for which special force-displacement laws, representing a wide range of possible structural behavior, have been assumed. The good agreement between the unknown parameters and the identified ones proved the capabilities of the proposed method. The robustness of the method has been also verified by contamination of the input data with artificial noises.

References

Belenky, V., Glotzer, D., Pipiras, V. and Sapsis, T.P. (2019), "Distribution tail structure and extreme value analysis of constrained piecewise linear oscillators", *Probab. Eng. Mech.*, **57**, 1-13.

Bernal, D. and Beck, J. (2004), "Special Structural Health monitoring benchmark, Section: Phase I of the IASC-ASCE", *J. Eng. Mech.*, **130**(1).

Boujo, E. and Noiray, N. (2017), "Robust identification of harmonic oscillator parameters using the adjoint Fokker-Planck equation", *Proceedings of the Royal Society A: Mathematical, Physical and Engineering Sciences*, **473**, 2200.

Breccolotti, M. and Materazzi, A.L. (2007), "Identification of a nonlinear spring through the Fokker-Planck equation", *Probab. Eng. Mech.*, **23**, 146-153.

Breccolotti, M., Materazzi, A.L. and Venanzi, I. (2008), "Identification of the nonlinear behaviour of a cracked RC beam through the statistical analysis of the dynamic response", *Struct. Control Health Monit.*, **15**, 416-435.

Cacciola, P. and Muscolino. G. (2002), "Dynamic response of a rectangular beam with a known non-propagating crack of certain or uncertain depth", *Comput. Struct.*, **80**, 2387-2396.

Cacciola, P., Impollonia, N. and Muscolino, G. (2003), "Crack detection and location in a damaged beam vibrating under white noise", *Comput. Struct.*, **81**, 1773-1782.

Chatzi, E.N. and Smyth, A.W. (2009), "The unscented Kalman filter and particle filter methods for nonlinear structural system identification with non-collocated heterogeneous sensing", *Struct. Control Health Monit.*, **16**, 99-123.

Chen, J. and Rui, Z. (2018), "Dimension-reduced FPK equation for additive white-noise excited nonlinear structures", *Probab. Eng. Mech.*, **53**, 1-13.

Doebling, S.W., Farrar, C.R., Prime, M.B. and Shevitz, D.W. (1996), *Damage identification and health monitoring of structural and mechanical system from changes in their vibrational characteristic: a literature review*. Los Alamos National Laboratories, Report LA-13070-MS, Los Alamos, New Mexico.

Erazo, K. and Nagarajaiah, S. (2018), "Bayesian structural identification of a hysteretic negati ve stiffness earthquake protection system using unscented Kalman filtering", *Struct. Control Health Monit.*, **25**, e2203.

Goldberg, D.E. (1989), *Genetic Algorithms in Search, Optimization and Machine Learning* Addison-Wesley.

Green, PL. (2015), "Bayesian system identification of a nonlinear dynamical system using a novel variant of Simulated Annealing", *Mech. Syst. Signal Pr.*, **52-53**, 133-146.

Hadjileontiadis, L.J., Douka, E. and Trochidis, A. (2005), "Crack detection in beam using kurtosis", *Comput. Struct.*, **83**, 909-919.

Hoon S, Farrar CR, Hemez FM, Czarnecki JJ, Shunk DD, Stinemates DW, Nadler BR. *A review of Structural Health Monitoring Literature: 1996-2001*. Los Alamos National Laboratories, Report LA-13976-MS, 2003, Los Alamos, New Mexico.

Hughes, T.J.R. (1987), *The Finite Element Method* Prentice Hall.

Iourtchenko, D.V., Mo, E. and Naess, A. (2006), "Response probability functions of strongly nonlinear system by the path integration method", *Nonlinear Mech.*, **41**, 693-705.

Kim, J.T. and Stubbs, N. (2003), "Crack detection in beam-type structures using frequency data", *J. Sound Vib.*, **259**, 145-160.

Lai, Z .and Nagarajaiah, S. (2019), "Sparse structural system identification method for nonlinear dynamic systems with hysteresis/inelastic behavior", *Mech. Syst. Signal Pr.*, **117**, 813-842.

Lai, Z. and Nagarajaiah, S. (2019), "Semi-supervised structural linear/nonlinear damage detection and characterization using sparse identification", *Struct. Control Health Monit.*, **26**, e2306.

Lei, Y. and Xia, D. and Erazo, K. and Nagarajaiah, S. (2019), "A novel unscented Kalman filter for recursive state-input-system identification of nonlinear systems", *Mech. Syst. Signal Pr.*, **127**, 120-135.

Li, H.N., Yi, T.H., Ren, L., Li, D.S. and Huo, L.S. (2014), "Reviews on innovations and applications in structural health monitoring for infrastructures", *Struct. Monit. Maint.*, **1**, 1-45.

Lin, H.P., Chang, S.C. and Wu, J.D. (2002), "Beam vibrations with an arbitrary number of cracks", *J. Sound*

Vib., **258**, 987-999.
Mosbah, H. and Fogli, M. (2003), "An original approximate method for estimating the invariant probability distribution of a large class of multi-dimensional nonlinear stochastic oscillators", *Probab. Eng. Mech.*, **18**(2), 165-170.
Neild, S.A., Williams, M.S, and McFadden, P.D. (2001), "Nonlinear vibration characteristic of damaged concrete beams", *J. Struct. Eng*., **129**(260), 260-268.
Owen, J.S., Eccles, B.J., Choo, B.S. and Woodings, M.A. (2001), "The application of auto-regressive time series modeling for the time-frequency analysis of civil engineering structures", *Eng. Struct.*, **23**(5), 521-536.
Patil, D.P. and Maiti, S.K. (2003), "Detection of multiple cracks using frequency measurements", *Eng. Fract. Mech.*, **70**, 1553-1572.
Petryna, Y.S. and Krätzig, W.B. (2005), "Compliance-based structural damage measure and its sensitivity to uncertainties", *Comput. Struct*., **83**(14), 1113-1133.
Piszczec, K. and Niziol, J. (1986), *Random Vibration of Mechanical System* Ellis Horwood Limited: Chichester.
Saavedra, P.N. and Cuitino, L.A. (2001), "Crack detection and vibration behaviour of cracked beams", *Comput. Struct.*, **79**(16), 1451-1459.
Shinozuka, M. and Jan, C.M. (1972), "Digital simulation of random processes and its application", *J. Sound Vib*., **25**, 111-128.
Von Wagner, U. and Wedig, W.V. (2000), "On the calculation of stationary solutions of multi-dimensional Fokker-Planck equations by orthogonal functions", *Nonlinear Dymam*., **21**, 289-306.
Wimarshana, B., Wu, N. and Wu, C. (2017), "Crack identification with parametric optimization of entropy & wavelet transformation", *Struct. Monit. Maint*., **4**(1), 33-52.
Wu, M. and Smyth, A.W. (2007), "Application of the unscented Kalman filter for real-time nonlinear structural system identification", *Struct. Control Health Monit*., **14**, 971-990.

SN